Applied Catalysis B: Environmental 111–112 (2012) 309–316

Contents lists available at SciVerse ScienceDirect

Applied Catalysis B: Environmental

journal homepage: www.elsevier.com/locate/apcatb

# Characterization and reactivity of $Al_2O_3$ supported Pd-Ni bimetallic catalysts for hydrodechlorination of chlorobenzene

N. Seshu Babu, N. Lingaiah*, P.S. Sai Prasad*

*Catalysis Laboratory, Inorganic & Physical Chemistry Division, Indian Institute of Chemical Technology, Hyderabad 500607, India*

ARTICLE INFO

*Article history:*
Received 26 July 2011
Received in revised form
23 September 2011
Accepted 6 October 2011
Available online 13 October 2011

*Keywords:*
Bimetallic Pd-Ni catalysts
Alumina
Deposition–precipitation
Hydrodechlorination
Chlorobenzene

ABSTRACT

A series of $Al_2O_3$ supported bimetallic Pd-Ni catalysts were prepared by deposition–precipitation method. The physico-chemical properties of the catalysts were evaluated by different characterization techniques such as temperature programmed reduction (TPR), temperature programmed desorption of $H_2$ (TPD), X-ray photoelectron spectroscopy (XPS), Braunner–Emmet–Teller (BET) surface area and pulse CO chemisorption. The activities of bimetallic Pd-Ni/$Al_2O_3$ catalysts were evaluated for continuous fixed bed gas phase hydrodechlorination of chlorobenzene operating at 140 °C under atmospheric pressure. The activity profiles demonstrate that an exceptional activity and stability of Pd-Ni/$Al_2O_3$ catalysts is accomplished by judicial variation of Ni composition with respect to Pd, which had arrived at Pd and Ni in 0.5:0.5 (wt%) ratio, while high Ni loaded Pd-Ni catalysts exhibit poorer stability. The high activity and stability of optimal catalyst is invoked due to formation of very active Pd-Ni interfaces embedded with $Pd^{\delta+}$ species, whereas lower stability resulted in high Ni loaded catalysts is due to aggregation of Ni component on topical Pd surface. The activity of mono and bimetallic catalysts are well correlate with the characterization results.



## 1. Introduction

Chlorinated hydrocarbons (CHCs) are widely used in many chemical industries as solvents, extractants, dry-cleaners, degreasing agents and specially adhesives due to their physical and chemical properties. Owing to their tremendous utilities in numerous commercial applications, CHCs are released into the environment in large quantities and constitute a very important environmental hazard [1]. Conventionally, abatement of the CHCs involves destructive technologies like incineration and thermal degradation, which often leads to the formation of carcinogenic byproducts. Thus, safe conversion of CHCs into value added products is still an intriguing goal of research. Catalytic hydrodechlorination (HDC) is identified as a promising non-destructive technique for detoxification of CHCs. It is safe, effective, economic, low energy demanding and environmentally benign for the removal of chlorinated wastes over conventional treatment methods [2]. Precious metals such as Pd [3–6] Pt [7] and Rh [8–11], Ni [12–15] catalysts either in bulk or supported form are widely used for the conversion of CHCs into safe products by catalytic HDC process under liquid and gas phase conditions. Of all, Pd is more active and selective than others metals [16]. A consensus emerging from the literature that HDC efficiency is sensitive to metal loading, nature of the support and with lower Pd [17] and Ni [18–20] dispersions. In addition, most of hydrogenolysis reactions are strongly influenced by the electronic structure of the active metal sites and method of catalyst preparation [21]. Previously, it was demonstrated that, an increase in activity and greater resistance to deactivation over larger Pd particles on $Nb_2O_5$ for HDC [22]. Nevertheless, the main problem associated with supported monometallic Pd catalysts is catalyst deactivation due to coke deposition [23], formation of surface metal halides [24,25], or metal sintering [26], which is a common feature of HDC systems. In recent article, it has been demonstrated that, the use of high surface area graphite as support material for Pd catalysts exhibit better stability as compare with conventional supports [5]. Several developments were made by concern with stability improvement of monometallic supported Pd catalysts by using proton scavengers, organic or inorganic base variants at various pH concentrations. However, these processes have been carried out under liquid phase conditions, therefore washing and activation procedures of catalyst is required for sequential runs [27,28]. Concern the adverse stability of monometallic catalysts, further research is explored on the modification of mono metallic catalytic systems by combining it with another transitional metal. In this regard, over the last few decades, there have been many improvements in the synthesis of heterogeneous bimetallic catalysts with well-designed structures. Indeed, unlike mono metallic Pd catalysts, new kinds of catalytic properties appeared in bimetallic catalysts due to synergetic

* Corresponding authors. Tel.: +91 40 27193163; fax: +91 40 27160921.
*E-mail addresses:* nakkalingaiah@iict.res.in (N. Lingaiah), saiprasad@iict.res.in (P.S. Sai Prasad).

0926-3373/$ – see front matter © 2011 Elsevier B.V. All rights reserved.
doi:10.1016/j.apcatb.2011.10.013

properties, as a consequence high activity and stability is achieved. In this context, several bimetallic catalysts such as Pd-Cu, Pd-Ag, Pt-Cu and Pt-V were explored for HDC reaction. These catalysts offered better stability as compared to monometallics [29]. In addition, an increase in catalytic HDC activity of chlorobenzene is observed with the addition of Fe to Pd/MgO and $Pd/Al_2O_3$ [30,31]. Many concepts with regard to electronic and geometric effects have been developed to elucidate the activity and stability of bimetallic catalysts for HDC is emerged. The catalysts prepared by modification of Pd by Fe, Co, Ni, Cr, and Cu supported on polyvinylpyrrolidine were studied in HDC of perchlorobenzene under liquid phase conditions [32]. It is suggested that, the formation of mixed oxide phase in bimetallic catalysts mutually prevents surface mobility of both the metals, which led to increased dispersion of the active metal component [33]. Besides, an improved activity and selectivity was observed in the gas phase HDC of chlorobenzene on $Pd\text{-}Rh/Al_2O_3$ due to electronic effects [34]. Simagina et al. studied Pd-Ni/C bimetallic catalysts for HDC of hexachlorobenzene under liquid phase conditions and inferred that efficacy of degree of dechlorination relies on surface Pd concentration in bimetallic Pd-Ni catalysts [35]. Recently, Pd on Ni-B nano particle catalysts has been reported for HDC of chlorobenzene under liquid phase conditions at 1 MPa $H_2$ pressure, where higher activity of Pd/Ni-B catalyst is invoked to the formation of Pd-Ni-B surface alloy upon heating [36].

Despite the formulations of myriad array of bimetallic catalysts, the existing database on HDC activities/selectivities for supported bimetallics is, insufficient to draw any generic conclusions. Nonetheless, it is generally acknowledged that catalytic HDC, is strongly influenced by the electronic structure of the active metal sites [37].

It is known that, the intrinsic disadvantage associated with catalysts prepared by conventional impregnation method is lack of uniform particle and distribution of active species because of forced condensation of metal precursors on the support, consequently limited activity results in any catalytic process. In contrast, deposition–precipitation (DP) is well-versed potential technique to avoid the drawbacks resulting from impregnation method, leading to development of high performance cost effective HDC catalysts.

Owing to high cost of Pd, it has become necessary to limit the loading of Pd for HDC reaction while rendering equal activity and stability like low dispersed Pd catalysts. Under this premise, previously we have reported that, supported Pd (1 wt%) catalysts prepared by deposition–precipitation method are found to exhibit greater chlorine tolerance, as a result, catalysts offered exceptional stability even better than low dispersed high loaded supported Pd catalysts. We reasoned that the high stability of DP catalysts is due to formation of an active electron deficient Pd species ($Pd^{n+}$) due to intimate metal–support interaction [38]. However, Pd loading below 1 wt% exhibits lower catalytic stability during time on stream HDC process due to insufficient concentration of support interacted Pd species and optimal Pd particle size [39,40]. Therefore, we envisioned that, coupling of Pd with appropriate transitional metal would impart new kind of catalytic species, which in turn shown notable chlorine tolerance in HDC reaction. The greater tolerance of chlorine species of bimetallic catalysts is due to either formation of alloy species or synergistic effect of bimetal. In this context, we sought to evaluate the effect of Ni composition on $Pd/Al_2O_3$ and their hydrodechlorination efficacy of chlorobenzene in continuous fixed bed reactor. At the outset of this study, an effort has been devoted to understand the variation of electronic properties of Pd species with inclusion of the Ni loading. Furthermore, activity and stability of these catalysts were well corroborated with various familiar characterization techniques such as TPR, TPD, XPS and EDAX. It is anticipated that, an electron donation from Pd to Ni could generate very active interfacial $Pd^{n+}$ species, an effect that is probed in this report.

## 2. Experimental

### 2.1. Catalyst preparation

The $Al_2O_3$ supported bimetallic Pd-Ni catalysts were prepared by deposition–precipitation method. The metal content of Pd is fixed at 0.5 wt% and the Ni loading is varied ranging from 0.25 to 2.0 wt%. In a typical method of catalyst preparation, a required quantity of $PdCl_2$ was dissolved in 1 M aq. HCl solution and to this solution, an appropriate quantities of aq. solution of $Ni(NO_3)_2$ were added. This bimetallic solution is further dispersed concurrently on γ-alumina support. To this catalyst mass, 1 M $Na_2CO_3$ was added slowly until $P^H$ of solution reached a value of 10.5, whereby $Pd(OH)_2$ and $Ni(OH)_2$ were exclusively precipitated on $Al_2O_3$ support. Then the solution left for 1 h in basic medium and washed the catalyst mass several times with deionised water until total chlorine was removed as confirmed by $AgNO_3$ test. The resultant catalysts were oven dried at 100 °C for 6 h and then calcined in air at 500 °C for 4 h. The catalysts were designated as Pd-0.5 (0.5 wt% Pd), PN-0.25, PN-0.5, PN-1, PN-2, Ni (2 wt% Ni), where numerical refers the Ni metal loading (wt%) in bimetallic catalysts.

### 2.2. Characterization of catalysts

XRD patterns were recorded on a Rigaku, Diffractometer, by using Ni-filtered $CuK_\alpha$ radiation ($\lambda = 1.5405$ Å). The measurements were recorded in steps of 0.045° with count time of 0.5 s in $2\theta$ range of 10–80°. Identification of the crystalline phases was made with the help of JCPDS files.

Temperature programmed reduction (TPR) of the catalysts was carried out in a flow of 10% $H_2$/Ar mixture gas at a flow rate of 30 ml/min with a temperature ramp of 10 °C/min. Before the TPR run the catalysts were pretreated in argon at 300 °C for 2 h. The hydrogen consumption was monitored using thermal conductivity detector of a gas chromatograph (Varian, 8301).

Temperature programmed desorption (TPD) of hydrogen of the catalysts was carried on the same instrument used for TPR studies. About 0.1 g of catalyst was placed in a quartz reactor. After reduction in $H_2$/Ar mixture (flow: 30 ml/min) at 300 °C for 1 h, the catalyst was flushed with Ar gas for 1 h at the same temperature to remove the physisorbed $H_2$. Then the sample was cooled in Ar flow and switch to continuing the gas flow of $H_2$/Ar at room temperature for a period of 30 min, ensuring the catalyst is saturate with $H_2$. The system was then purged with Ar flow (30 ml/min) to remove physisorbed $H_2$ and TPD of $H_2$ was monitored while raising the catalyst temperature at a rate of 10 °C/min from 30 to 800 °C. The amount of desorbed hydrogen was determined by gas chromatography using a thermal conductivity detector.

Room temperature CO chemisorption was carried out on a pulse adsorption apparatus. In a typical experiment, the catalyst was first oxidized in a 10% $O_2$/He mixture at 300 °C for 30 min and subsequently reduced in 10% $H_2$/He gas at the same temperature, flushing with pure He in between. The CO adsorption capacity was then obtained by the number of pulses required to saturate the total surface of the catalyst.

The specific surface areas of the catalyst samples were estimated using $N_2$ adsorption at −196 °C by the single point BET method using Micromeritics Pulse Chemisorb 2700. Prior to BET measurement, the samples were dried at 150 °C for 2 h.

XPS measurements were conducted with a KRATOS AXIS 165 with a DUAL anode (Mg and Al) apparatus using the $MgK_\alpha$ anode. The non-monochromatized Al-$K_\alpha$ X-ray source ($h\nu = 1486.6$ eV) was operated at 12.5 kV and 16 mA. Before acquisition of the data the sample was out gassed for about 3 h at 100 °C under a pressure of $1.0 \times 10^{-2}$ Torr to minimize surface contamination. The XPS instrument was calibrated using Au as a standard material. For

energy calibration, the carbon 1s photoelectron line was used. The carbon 1s binding energy was taken as 285 eV. Charge neutralization of 2 eV was used to balance the charge up of the sample. The spectra were deconvoluted using Sun Solaris based Vision-2 curve resolver. Binding energies for identical samples were, in general reproducible within ±0.1 eV.

### 2.3. Activity measurements

The HDC reaction was performed under atmospheric pressure at 140 °C. In a typical experiment about 0.8 g of catalyst was suspended between two quartz wool plugs of glass reactor (12 mm) and reduced in a flow of hydrogen (30 ml/min) at 300 °C for 2 h prior to the reaction. After bringing the temperature of the catalyst bed to the required level (140 °C), chlorobenzene was fed by means of a microprocessor based feed pump (Braun Corp, Germany) at a flow rate of 4 ml/h in to the preheater portion of the reactor, where layer of glass beads sieved of same size with catalyst particle size, placed to facilitate vaporization of feed component before reaching catalyst zone, ensuring negligible heat and mass transfer limitations. The particle size of catalyst was fixed below a value sieved with BSS 85/100 of mesh size based on the influence of initial reaction rate, ensuring the reaction under chemical control regime [41]. The $H_2$ flow was kept at a molar ratio of $H_2$ to chlorobenzene of 3:1. The products were collected at the down flow of the reactor by keeping low temperature trap and analyzed by gas chromatography using a FID detector with 10% carbowax 20 M column. The results generated during HDC study are reproducible within ±3% with the same batch of catalysts used for separate experiments.

The percentage conversion of chlorobenzene was defined as follows, % Conversion of chlorobenzene = 100 (moles of chlorobenzene fed − moles of chlorobenzene remaining)/moles of chlorobenzene fed

## 3. Results and discussion

### 3.1. X-ray diffraction studies

XRD patterns of pre-reduced Pd-Ni/$Al_2O_3$ catalysts exhibited diffraction lines are related to alumina support only and no indication of presence of any metallic or alloy phases of Pd and Ni (Figure not shown). As alumina is amphoteric in nature and loading of Pd and Ni precursors are too low, thus both metal species are dispersed uniformly on $Al_2O_3$ with consequent generation of smaller particles. In general, XRD shows diffraction lines of metal phases having the particle size > 4 nm only. This observation made in line with literature report that, a metal can disperse on the surface of another metal to form highly dispersed bimetallic system particularly at Pd loading <2 wt% [42].

### 3.2. Temperature programmed reduction

TPR profiles of mono and Ni containing bimetallic Pd/$Al_2O_3$ catalysts are shown in Fig. 1. The TPR patterns of Pd/$Al_2O_3$ catalyst featured with low temperature reduction signal centered at 100 °C pertinent to reduction of weak interacted PdO to Pd, while a broad reduction signal appears at $T_{max}$ 350–550 °C is attributed to the reduction of subsurface PdO species. The formation of subsurface PdO species is usually noticed in low concentrated high dispersed alumina supported Pd catalysts [43].

In marked contrast, TPR profiles of Pd-Ni/$Al_2O_3$ catalysts displays two distinct reduction peaks within $T_{max}$ 100–200 °C. The low temperature signal is pertinent to reduction of weakly interacted PdO species to Pd, while reduction curve shown at $T_{max}$ 180 °C, is could be due to reduction of strong interacted PdO species with Ni surface planes. This effect is pronounced in presence of Ni containing Pd/$Al_2O_3$ catalysts, particularly in low Ni loaded Pd/$Al_2O_3$ catalysts. The disparity in reduction behavior of mono and bimetallic catalysts is presumably due to difference in metal–metal/metal–support interaction and Ni composition as well. As the catalysts are prepared by DP method, an intimate metal–support/metal–metal interaction anticipated which leads to formation of $Pd^{\delta+}$ species.

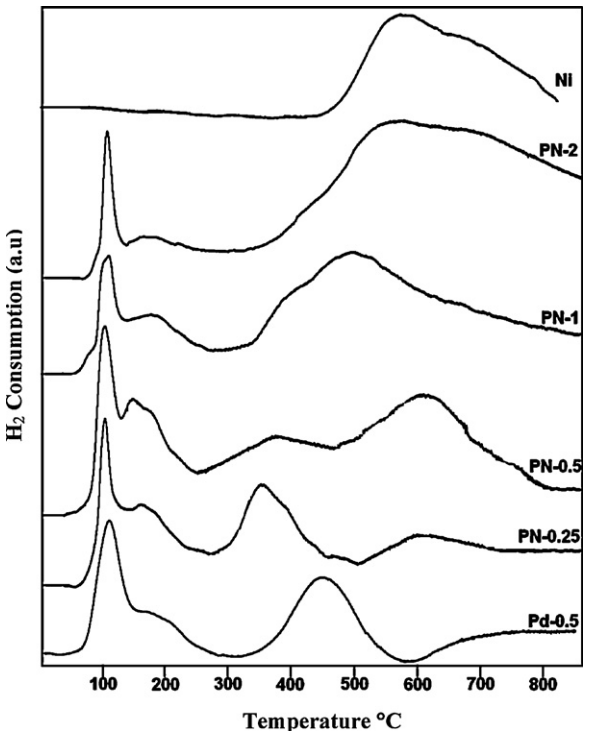


**Fig. 1.** Temperature programmed reduction patterns of Pd-Ni/$Al_2O_3$ catalysts.

Table 1 illustrates the actual amount of hydrogen consumed is estimated by integrating each reduction signal. The results inferred that propensity of Pd species that interacted with support/Ni surface increases gradually with increase in Ni loading up to 0.5 wt% (PN-0.25 and PN-0.5) and then decreased. As Ni loading increases beyond 0.5 wt%, distribution of surface NiO species are more oppress over surface PdO on $Al_2O$, eventually weak Pd-support/Pd-Ni interaction took place. As a result, featureless reduction signal is noticed pertinent to surface interacted PdO at $T_{max}$ 180 °C in TPR profiles. Notably, $H_2$ consumption estimated at $T_{max}$ 180 °C recorded as higher for PN-0.5 catalyst as compared to PN-1 and PN-2 catalysts (20.7 μmol/gm for PN-0.5 vs 4.9 μmol/gm for PN-2). Furthermore, no negative $H_2$ consumption peak due to decomposition of β-PdH a characteristic of large Pd particles is observed for all the catalysts [40]. It is noteworthy that the absence of such negative reduction peak is evident the formation of smaller Pd particles in all cases, which is due to low concentration of Pd. In addition, there

**Table 1**
$H_2$ consumption of Pd-Ni/$Al_2O_3$ catalysts determined by TPR measurements.

| Catalyst | $T_{max}$ of $H_2$ consumption (μmol/gm) | | |
|---|---|---|---|
| | 100 °C | 160–200 °C | $[PdO]_{SC}$ |
| Pd-0.5 | 29.4 | 3.7 | 13.8 |
| PN-0.25 | 23.8 | 13.3 | 9.8 |
| PN-0.5 | 26.6 | 20.7 | 2.9 |
| PN-1 | 39.3 | 7.6 | – |
| PN-2 | 43.7 | 4.9 | – |
| Ni | – | – | – |

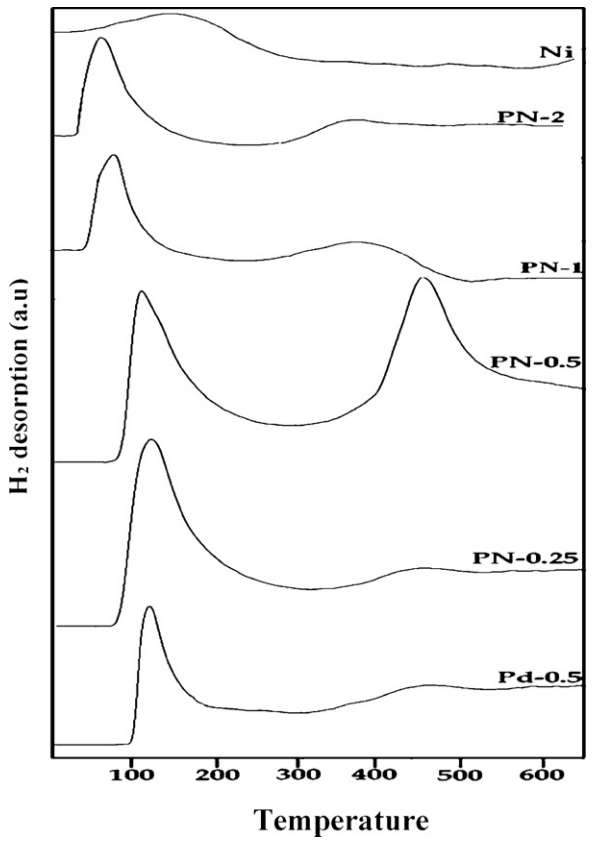


**Fig. 2.** Temperature programmed desorption of hydrogen patterns of Pd-Ni/$Al_2O_3$ catalysts.

is considerable decrement in intensity and reduction temperature of subsurface PdO species from 450 °C in Pd-0.5 to 350 °C in case of PN-0.25 and PN-0.5 catalysts. This suggests that tendency of subsurface PdO species formation is decreased in case of PN-0.25 and PN-0.5 catalysts. Whereas, there is no subsurface PdO is identified in PN-1 and PN-2 implying a weak Pd-support interaction.

Besides these Pd reduction signals, TPR profiles are also characterize with a broad high temperature $H_2$ consumption peak in Pd-Ni/$Al_2O_3$ and Ni/$Al_2O_3$ catalysts appears at $T_{max}$ of 350–600 °C, which attributes to the reduction of fixed NiO species or support interacted NiO [44]. In general, Ni form spinal type species $NiAl_2O_4$ with $Al_2O_3$ support and these species reduced at higher temperatures [45]. In literature, it has been reported that, TPR patterns are influenced by metal/support interaction, which in turn are sensitive to metal loading, catalyst preparation and pretreatment [46]. As the loading of Ni increased from 025 to 2 wt%, there is a decrease in reduction temperature of NiO, where Ni-support interaction is stronger at lower Ni loading and such effect is decreased with increase in metal loading.

### 3.3. Temperature programmed desorption of $H_2$

Hydrogen temperature-programmed desorption can provide some light on differences in metal/support interaction and electronic properties of supported metal particles [47,25]. A direct comparison of the $H_2$ TPD profiles generated in this study with the limited reports in the literature relating to supported Pd systems is problematic given the differences in metal loading/support/preparation/activation/desorption procedures. The $H_2$ TPD profiles are presented in Fig. 2, pertinent to $H_2$ release and $T_{max}$ values. Each desorption profile constitute a common desorption peak at $T < 120$ °C, is due to release of chemisorbed $H_2$ from

**Table 2**
$H_2$ desorption of bimetallic Pd-Ni catalysts determined by TPD measurement.

| Catalyst | $H_2$ desorption (μmol/gm) | |
|---|---|---|
| | $T_{max}$ (120–150 °C) | $T_{max}$ (450–480 °C) |
| Pd-0.5 | 20.2 | – |
| PN-0.25 | 24.2 | 4.7 |
| PN-0.5 | 26.1 | 10.2 |
| PN-1 | 9.7 | 3.2 |
| PN-2 | 7.1 | 2.4 |
| Ni | – | – |

Pd surface. Similar observation of removal of $H_2$ from Pd/$SiO_2$ at 0–227 °C is reported in literature [48]. Uptake of $H_2$ on Ni/$Al_2O_3$ was considerably low to that delivered by Pd/$Al_2O_3$, therefore no measurable desorption signal is noticed on Ni/$Al_2O_3$ catalyst due to partial reduction of NiO species on $Al_2O_3$. Besides, each profile characterized with presence of discernible higher-temperature release of $H_2$ in the range of $T_{max}$ 400–450 °C for all bimetallic catalysts, albeit with different intensities. It is intriguing to note that, a broad and intense signal associate with PN-0.5 catalyst appears due to formation of Pd-Ni ensembles, which in turn due to an intimate metal–metal interaction during DP method of catalyst preparation. These sites could be invoked to the evolution of hydrogen at $T_{max}$ 400–450 °C. It can be perceived that $H_2$ spillover effect may cause for the presence of high temperature desorption peak. Being Pd is in reduced state, where the adsorbed $H_2$ species on Pd surface is split into the H atoms, and then transport to metal–support/metal–metal interface, where H atoms are recombine into $H_2$ with subsequent evolution of $H_2$ upon heating. The amount of spillover proportionate to degree of bimetal interfaces, which in turn rely upon the amount of Ni loading. The better bimetal interface arrived at Pd-Ni (0.5:0.5 wt%) and then decreased beyond 0.5 wt% Ni. The estimation of area of individual signal reveals that, $H_2$ desorption by PN-0.5 catalyst is appreciably higher than that delivered by any other current disclosed catalysts. Table 2 illustrates that, $H_2$ liberated by monometallic Pd/$Al_2O_3$ catalyst is 20 μmol/g, which is far inferior to that delivered by PN-0.5 (26.1 mol/g at <120 °C, and 10.2 μmol/g at $T_{max}$ 400–450 °C). In marked contrast, PN-1 and PN-2 catalysts evolved considerable lower amount of both chemisorbed and spillover $H_2$, due to poor abundance of dispersed Pd species, because of surface segregation of Ni species at high Ni loadings.

Literature precedents reveal that, disparity in amount of $H_2$ spillover associate with different supported metal systems or metal on the same support is reported. Furthermore, there are many factors influence the $H_2$ spillover such as nature of hydrogen donor, activation temperature, degree of metal dispersion. Having these amenable factors, it is strive to interrelate and explicate any of these factors ascertain to spill over. The current results demonstrate quite different behavior for both mono and bimetallic Pd/$Al_2O_3$ catalysts, where amount of spillover is relying on the Ni composition and degree of metal–metal/metal–support interaction [49–51].

### 3.4. BET surface area and pulse CO chemisorption

The physico-chemical properties of catalysts are shown in Table 3. The surface area of $Al_2O_3$ support was 210 $m^2$/gm. The metal loaded alumina exhibited lower surface area compared with the support alone. However, there is no marginal variation in support surface area up to 0.5 wt% of Ni loading, whereas support surface area decreased significantly in high Ni loaded bimetallic Pd-Ni catalysts (PN-1 and PN-2). The decrease in surface area of these catalysts presumably relate to partial destruction of the support ordering or due to obstruction of the pore entrances.

**Table 3**
Physico-chemical properties of mono and bimetallic Pd-Ni/$Al_2O_3$ catalysts.

| Catalyst | Pd content (wt%) (ICP) | Ni content (wt%) (ICP) | Surface area ($m^2$/gm) | CO uptake (ml/gm) |
|---|---|---|---|---|
| $Al_2O_3$ | – | – | 210 | – |
| Pd-0.5 | 0.45 | – | 209 | 0.86 |
| Ni | – | 1.7 | 159 | 0.09 |
| PN- 0.25 | 0.47 | 0.19 | 196 | 0.82 |
| PN-0.5 | 0.44 | 0.42 | 193 | 0.79 |
| PN-1 | 0.38 | 1.2 | 150 | 0.63 |
| PN-2 | 0.40 | 1.7 | 114 | 0.50 |

Pulse CO chemisorption data of alumina supported bimetallic Pd-Ni catalysts are also shown in Table 3. It is obvious that, monometallic Pd/$Al_2O_3$ catalyst exhibited higher CO adsorption as compared to bimetallic Pd-Ni catalysts due to dilution of active component by the presence of Ni ensembles. The high dispersion of the monometallic Pd catalysts can be attributed to the strong metal–support interaction during the DP method of catalyst preparation [51–54]. However, CO uptake is decreased progressively with increase in Ni composition of bimetallic catalysts.

### 3.5. X-ray photoelectron spectroscopy (XPS)

XPS analysis can be helpful to understand the nature of electronic properties of bimetals. The XPS spectra pertains the binding energy (B.E) of Pd of pre-reduced and used catalysts are presented in Fig. 3a, and b, respectively. The values of binding energies of Pd $3d_{5/2}$ and Ni $2p_{3/2}$ are shown in Table 4. In case of pre-reduced catalysts (Fig. 3a), the Pd $3d_{5/2}$ B.E of Pd/$Al_2O_3$ catalyst is recorded as 336.2 eV, this value is higher than the B.E of metallic Pd due to existence of electron deficient Pd species ($Pd^{n+}$) generated as result of strong metal–support interaction during DP method of preparation [41–43]. On the other hand, Pd $3d_{5/2}$ B.E of Pd-Ni catalysts recorded as 336.5 for PN-0.25. Interestingly, B.E of core level Pd $3d_{5/2}$ in PN-0.5 is deconvoluted into two, one is centered at 336.0, and 336.9 eV, the former corresponds to weak support interacted Pd species, while latter pertinent to $Pd^{\delta+}$ species. The more positive shift in Pd $3d_{5/2}$ B.E for PN-0.5 relative to the Pd/$Al_2O_3$ catalyst is attributed to formation of Pd-Ni interface on $Al_2O_3$. Similar enhancement of Pd 3d B.E is also evident from literature that, the shift in Pd $3d_{5/2}$ B.E to higher for the bimetallic Ni-Pd nanocatalyst relative to that for the monometallic Pd sample, while the shift of Ni $2p_{3/2}$ levels to lower energies relative to the monometallic Ni sample [52]. In another report, it was demonstrate that same observation of incremental effect of Pd $3d_{5/2}$ binding energy of Pd-Pt bimetallic catalyst [53]. The increased Pd $3d_{5/2}$ B.E is possibly arouse due to electronic relaxation energy of Pd levels in the presence of Ni. As a result, it is assumed that a close contact between Pd and Ni (not alloy) may account for higher Pd $3d_{5/2}$ binding energy. On the other hand, surface Pd species were not traced in PN-1 and PN-2 during XPS analysis, which thought to be surface segregation of Ni atoms on the Pd species at higher Ni loadings.

**Table 4**
XPS data of bimetallic Pd-Ni/$Al_2O_3$ catalysts.

| Catalyst | Binding energy (eV) | | | | Post-HDC EDX | |
|---|---|---|---|---|---|---|
| | Pre-HDC | | Post-HDC | | Cl/Pd | Cl/Ni |
| | Pd $3d_{5/2}$ | Ni $2P_{3/2}$ | Pd $3d_{5/2}$ | Ni $2P_{3/2}$ | | |
| Pd-0.5 | 336.1 | – | 337.7 | – | 7.4 | – |
| PN-0.25 | 336.5 | 855.6 | 337.0 | 856.5 | 3.5 | 8.1 |
| PN-0.5 | 336.7 | 855.4 | 336.8 | 856.8 | 3.0 | 9.3 |
| PN-1 | – | 855.8 | – | 856.3 | – | 8.6 |
| PN-2 | – | 855.9 | – | – | – | 8.2 |
| Ni | – | 856.0 | – | – | – | – |

Some consensus emerging form literature is that, an increase in the Pd core electron energy of about 0.5 eV was measured for Pd on Ni crystals for which Pd retained compressive strains [54]. However, reconstructions occurred on extended surfaces, which may not have been the case for small particles. Nevertheless, it is known that compressive strains induce an increase of the *d*-band width, which would be expected to lead to a downshift in the gravity centre of the *d*-band, that is, toward higher binding energy [55].

The Ni $2P_{3/2}$ binding energy for pre reduced Ni/$Al_2O_3$ catalyst at 300 °C is shown in Fig. 3c. It is known that the binding energy of Ni $2p_{3/2}$ for metallic Ni and NiO species observed at 852.0 and 856.0 eV, respectively [56]. In the present case, Ni $2p_{3/2}$ binding energy of reduced PN-0.25 and PN-0.5 catalysts observed as 855.6 and 855.4 eV, respectively, while Ni $2p_{3/2}$ binding energy for PN-1 and PN-2 catalysts observed at 855.8 and 855.9 eV, respectively. However, in the present case, B.E for Ni/$Al_2O_3$ catalyst close to B.E of NiO species (Table 3), which is due to the fact that NiO species not reduced completely at 300 °C, as indicated by TPR measurements. The minimal negative shift in Ni $2p_{3/2}$ B.E of PN-0.25 and PN-0.5 catalysts compared to B.E of Ni in Ni/$Al_2O_3$ is attributed to fraction of electron density transfer from Pd to Ni species. This observation is in line with literature report [51,53].

### 3.6. Activity measurements:

The catalytic activity of Pd/$Al_2O_3$ and Pd-Ni/$Al_2O_3$ catalysts were evaluated for the gas phase hydrodechlorination of chlorobenzene operating at 140 °C under atmospheric pressure. The activity profiles (Fig. 4) demonstrate that all the catalysts, except Ni/$Al_2O_3$, were showing similar HDC conversions at initial reaction time; however, their activity trend varied as reaction time proceeds. First of all, despite of having highly dispersed Pd species, Pd-0.5 catalyst displayed adverse catalytic stability during the course of reaction. This is might be due to insufficient concentration of active Pd component for attaining steady state activity [39,40]. Deactivation of the catalyst for HDC reaction mainly due to carbon deposition/aggregation of the active metal sites, surface poisoning by HCl and/or metal sintering [57]. The monometallic Ni/$Al_2O_3$ catalyst displays negligible HDC conversion of chlorobenzene under the defined reaction conditions. It is known that supported Ni based catalysts are HDC active at considerable high temperatures relative to Pd counterparts.

The HDC reactivity and stability trend of bimetallic catalysts can be illustrated as PN-0.5 > PN-0.25 > Pd-0.5 ~ PN-1 > PN-2 > Ni under the stated reaction conditions. There are several factors influencing the activity of bimetallics is that, (i) are the two elements may intimately interacting in the same aggregates? (ii) does the surface segregation of one component occur? (iii) are the two elements randomly distributed in the surface layer or not? [58]. The first and second points rely upon the method of catalyst preparation and third may be concerns the surface composition in bimetallic particles. As like Pd/$Al_2O_3$, PN-1 and PN-2 catalysts are also prone to be deactivated during HDC of chlorobenzene, albeit slowly. The lower catalytic stability of PN-1 and PN-2 catalysts is attributed to the surface segregation of Ni species on

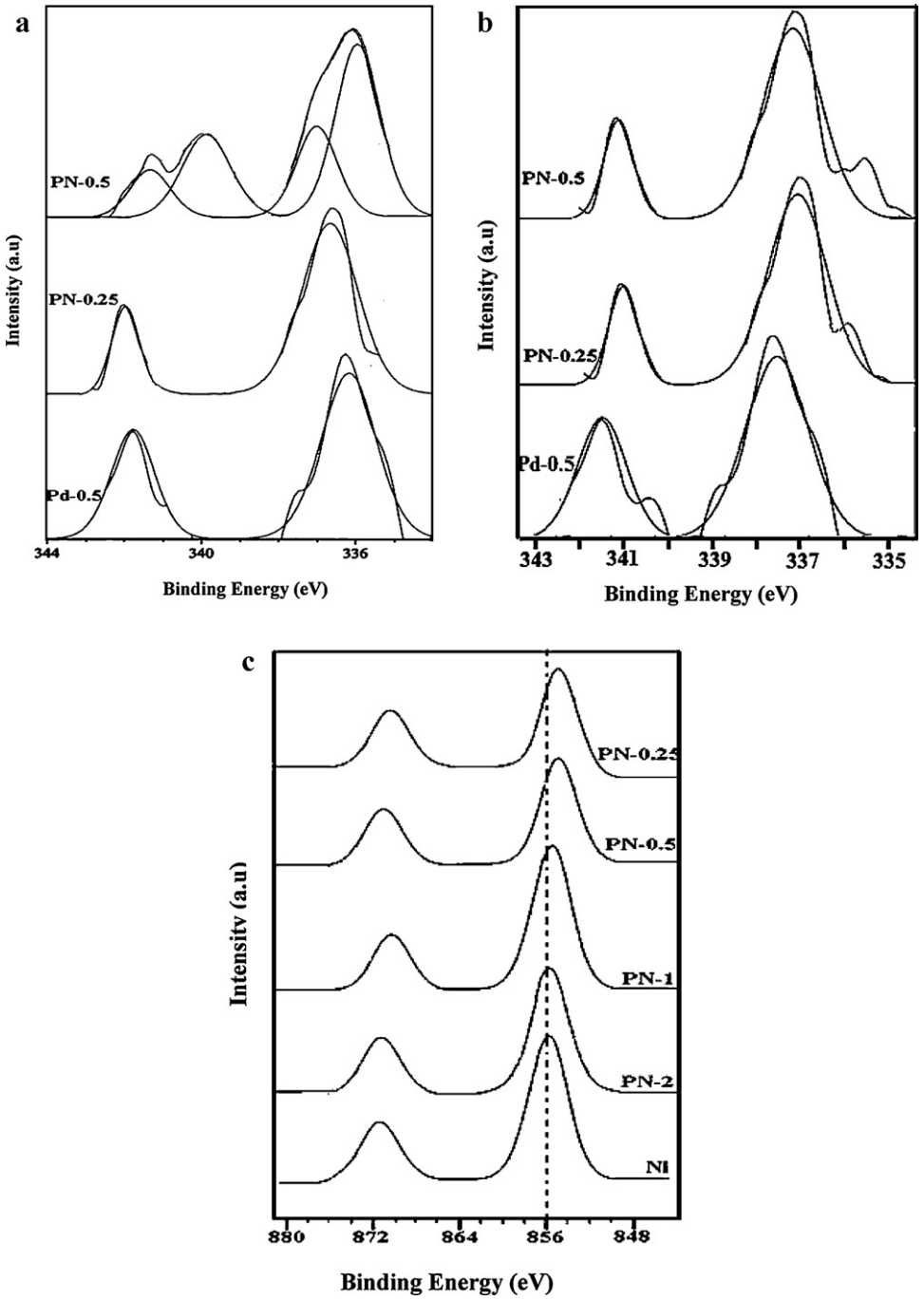


**Fig. 3.** (a) XPS spectra of reduced catalysts pertain to Pd binding energy. (b) XPS spectra post HDC catalysts pertain to Pd binding energy. (c) XPS spectra reduced catalysts pertain to Ni binding energy.

Pd surface, thereby accessibility of active Pd species are limited. TPR measurements also provide us good consensus with aforementioned observations that, reduction temperature of NiO in PN-1 and PN-2 catalysts is decreased marginally due to weak metal–metal/metal–support interaction. Furthermore, it is apparent that, as Ni loading increased on $Pd/Al_2O_3$, the corresponding metal surface composition increased as evidenced by the absence of surface Pd species during XPS measurements. Notably, PN-0.5 displayed venerable HDC activity and stability throughout period of 15 h as compared to high Ni loaded $Pd/Al_2O_3$ catalysts and monometallic $Pd/Al_2O_3$ as well. The situation is more complex to analyze here with bimetallic catalysts, especially because the dispersion has effect on the surface composition. Indeed it appears that catalysts with similar surface compositions (Pd-Ni-0.5) exhibit higher activity regardless of the lower dispersions (Fig. 1). A close look at the steady state activity of bimetallic catalysts reveals that, PN-0.25 shown consistent activity up to 12 h and then decreased slightly. The reason for lower stability of PN-0.25 relative to PN-0.5 catalyst is attributed to difference in contact between Pd and Ni metals, where part of Pd remains isolated without being interacted with Ni.

Furthermore, high activity and stability of bimetallic catalysts can be explained due to one of the following or combined effects (i) electronic effects, (ii) geometric effects, (iii) occurrence of mixed oxide sites, (iv) disappearance of β-PdH phase [58]. It is well known that some classes of reaction are more or less sensitive to some of

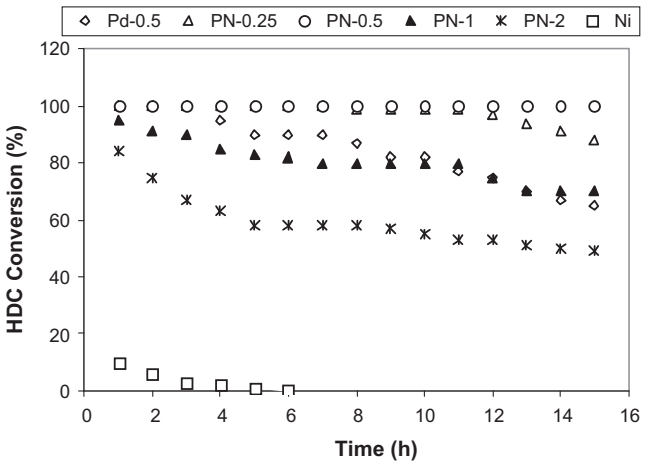


**Fig. 4.** Activity profiles of Pd-Ni/$Al_2O_3$ catalysts.

these factors. For instance electronic factors play a discernible role in the selective hydrogenation of unsaturated hydrocarbons, while geometric effects are prevailing in the hydrogenolysis of alkanes. Nonetheless, in the present case, an electronic effect predominates due to metal–support/metal–metal interaction, but not an alloy or β-PdH phase formation. TPR profile indicated that, there is significant decrease in reduction temperature of subsurface PdO species together with generation of highly interacted Pd species associated with NiO species. TPD results manifest the observation made by TPR patterns that, presence of high temperature desorption peak associate with PN-0.5 catalyst at $T_{max}$ 400–500 °C is due to evolution of $H_2$ from Pd-Ni interface. In addition, some negative charge transfer from Pd to Ni in PN-0.5 is observed by XPS, which indicates strong electronic forces exist between two metals. Prablo Argentiere and Nora Figoli [59] claimed that the increase in Pd $3d_{5/2}$ B.E in Pd-Co and Pd-W catalysts suggests an electron transfer from Pd to Co and W, rather than Pd-Co and Pd-W bonds formation. In the present case also, it appears that a discernible increment in Pd $3d_{5/2}$ B.E of PN-0.5 catalyst is due to formation of Pd-Ni interfaces embedded with $Pd^{\delta+}$ species, which are more active for the HDC reaction. The involvement of spill over $H_2$ in catalytic HDC [60] is further considered where the nature of accepting oxide support can have a significant influence on hydrogen transfer even in the presence of surface chlorine [61]. However, in the present case, surface chlorine is totally removed during DP method; therefore presence of spill over $H_2$ contributes to the HDC activity is mainly due to improved metal–support/metal–metal interaction.

Furthermore, nature of support plays a significant role in HDC reaction [62]. The occurrence of hydrogen spillover may be due to synergetic effect, which has a role to play in catalytic HDC. The $Pd^{\delta+}$ species generated due to formation of Pd-Ni interfaces in PN-0.5 catalyst were stabilized in the vacant octahedral holes on the alumina support [63]. Alumina unlike other supports, has unoccupied octahedral sites and therefore it assumed that on the surface of $Al_2O_3$ the top $O^{2-}$ ion of the octahedron is missing, the remaining part of $O^{2-}$ skeleton forms a square pyramid. Therefore, the stabilization of the cationic Pd appears to be more favorable on alumina. It is reiterating that, catalytic HDC is strongly influenced by the method of catalyst preparation, the nature of support [64], the extent of metal loading [40,65], dispersion [66] and the presence of a second metal [67–69].

Therefore, it is apparent that, the adequate presence of Pd and Ni component on $Al_2O_3$ support prepared by DP method offers strong metal–support/metal–metal interaction, reached maximum at particular bimetal composition of Pd-Ni (0.5:0.5 wt%). While, in case of high Ni loaded PN-1 and PN-2 catalysts, abundance of surface interacted Pd species are scarce, as indicated by XPS measurements, consequently catalyst activity is dropped continuously.

The plausible HDC mechanism on catalytic surface illustrated as, C–Cl bond of chlorinated aromatics acquires double bond character due to loss of Cl p-electrons due to resonance. Following this, formation of diadsorbed chloroaromatic species derived from the adsorption of chloro aromatic compounds on Ni and Pd, which are eventually attacked by hydride ions. To end HDC cycle, above step leads to generation of adsorbed phenyl anions, which then accepts protons to form benzene [70].

Post HDC catalysts are characterized with surface techniques to know the influence of intrinsic chlorine adsorption on the catalyst surface during the HDC reaction. XPS results of post HDC catalysts reveal that (Table 3), B.E of Pd $3d_{5/2}$ in PN-0.5 catalysts remains same as that of pre-HDC catalyst, whereas there is discernible increase in Ni $2p_{3/2}$ B.E of post HDC counterparts. The reason for increase in Ni $2p_{3/2}$ B.E is suggests that, chlorine released during HDC reaction is easily attacked by Ni species rather they bound to Pd surface. The tendency of Ni surface to chlorine is highest in case of PN-0.5 catalyst, where Pd is in Pd-Ni interface embedded with highly electron deficient state. This observation is further substantiated by the surface composition of pre and post HDC catalysts as measured by EDAX technique. This data reveals that, Cl/Pd ratio is recorded higher (7.4) in case of monometallic Pd/$Al_2O_3$ catalysts, while it is recorded as lowest (3.0) in case of PN-0.5. It is noteworthy that, Cl/Ni ratio is recorded as high as 9.3 for PN-0.5 as compared to other of PN counter parts. However, there is decreased value of Cl/Ni ratio in case of PN-1 and PN-2 catalysts because of lower catalytic activity, therefore degree of chlorine release is decreased. It is apparent that, electron deficient Pd particles are more chlorine tolerant due to electrophilic character of chlorine, as a result poisoning of catalyst surface is reduced significantly.

Therefore, an improved performance of PN-0.5 catalyst could be due to both structural and electronic effect regardless of degree of metal dispersion. Also, a measurable enhancement in HDC performance of PN-0.5 must be result of some surface synergy between Pd and Ni, and higher $H_2$ association with PN-0.5 catalyst as well. In HDC applications over supported bimetallics [71], a close contact between Pd and second metal (not alloy formation) has been deemed to be essential for significant catalytic activity. The Pd component directly activate C–Cl bond with subsequent attack from reactive hydrogen associated at the Ni centers.

## 4. Conclusions

In summary, it is documented yet another remarkable stable bimetallic Pd-Ni (PN-0.5) catalyst for gas phase HDC of chlorobenzene. Among all, PN-0.5 catalyst displays venerable chlorine tolerance and consistent activity during time on stream analysis of HDC of chlorobenzene. The judicial selection Pd and Ni composition on $Al_2O_3$ is a pivotal factor for the superior performance of the bimetallic. The exceptional activity of PN-0.5 cannot be ascribed either due to the independent effect of Ni or Pd. The electronic effects are more prevailed for superior performance of PN-0.5 catalyst, wherein maximum interaction between Pd and Ni species took place with consequent generation of Pd-Ni interface species.

## References

[1] E. Goldberg, Sci. Total Environ. 100 (1991) 17–28.
[2] T.N. Kalnes, R.B. James, Environ. Prog. 7 (1988) 185–191.
[3] B.T. Meshesha, R.J. Chimentão, A.M. Segarra, J. Llorca, F. Medina, B. Coq, J.E. Sueiras, Appl. Catal. B: Environ. 105 (2011) 361–372.
[4] E. Díaz, L. Faba, S. Ordóñez, Appl. Catal. B: Environ. 104 (2011) 415–417.
[5] E. Díaz, S. Ordóñez, R.F. Bueres, E. Asedegbega-Nieto, H. Sastre, Appl. Catal. B: Environ. 99 (2010) 181–190.
[6] T. Janiak, J. Okal, Appl. Catal. B: Environ. 92 (2009) 384–392.

[7] M. Bonarowska, Z. Kaszkur, L. Kępiński, Z. Karpiński, Appl. Catal. B: Environ. 99 (2010) 248–256.
[8] B. Coq, G. Ferrat, F. Figueras, J. Catal. 101 (1986) 434–445.
[9] S. Ordóñez, H. Sastre, F.V. Díez, Appl. Catal. B: Environ. 40 (2003) 119–130.
[10] Y. Amenomiya, V.I. Birss, M. Goledzinowski, J. Galuszka, A.R. Singer, Catal. Rev. Sci. Eng. 32 (1990) 163–227.
[11] E. Diaz, A.F. Mohedano, J.A. Casas, L. Calvo, M.A. Gilarranz, J.J. Rodriguez, Appl. Catal. B: Environ. 106 (2011) 469–475.
[12] S. Ordóñez, H. Sastre, F.V. Díez, React. Kinet. Catal. Lett. 70 (2000) 61–66.
[13] E.J. Shin, M.A. Keane, J. Catal. 173 (1998) 450–459.
[14] J.-T. Feng, Y.-J. Lin, D.G. Evans, X. Duan, D.-Q. Li, J. Catal. 266 (2009) 351–358.
[15] W. Wu, J. Xu, R. Ohnishi, Appl. Catal. B: Environ. 60 (2005) 129–137.
[16] J.C. Bertolini, Y. Jugnet, in: D.P. Woodruff (Ed.), Alloy Surfaces and Surface Alloys, 10, Elsevier, Amsterdam, 2002, pp. 404–437.
[17] W. Juszczyk, A. Malinowski, Z. Karpiński, Appl. Catal. A: Gen. 166 (1998) 311–319.
[18] A.R. Suzdorf, S.V. Morozov, N.N. Anshits, S.I. Tsiganova, A.G. Anshits, Catal. Lett. 29 (1994) 49–55.
[19] G. Pina, C. Louis, M.A. Keane, Phys. Chem. Chem. Phys. 5 (2003) 1924–1931.
[20] M.A. Keane, C. Park, C. Menini, Catal. Lett. 88 (2003) 89–94.
[21] A.Yu. Stakheev, L.M. Kustov, Appl. Catal. A: Gen. 188 (1999) 3–35.
[22] R. Gopinath, K.N. Rao, P.S. Sai Prasad, S.S. Madhavendra, S. Narayanan, G. Vivekanandan, J. Mol. Catal. A: Chem. 181 (2002) 215–220.
[23] E.J. Creyghton, M.H.W. Burgers, J.C. Jansen, H. Van Bekkum, Appl. Catal. A: Gen. 128 (1995) 275–288.
[24] J. Estellé, J. Ruz, Y. Cesteros, R. Fernandez, P. Salagre, F. Medina, J.E. Sueiras, J. Chem. Soc. Faraday Trans. 92 (1996) 2811–2816.
[25] C. Park, C. Menini, J.L. Valverde, M.A. Keane, J. Catal. 211 (2002) 451–463.
[26] D.A. Dodson, H.F. Rase, Ind. Eng. Chem. Prod. Res. Dev. 17 (1978) 236–240.
[27] M. Cobo, J.A. Conesa, C.M. de Correa, Appl. Catal. B: Environ. 92 (2009) 367–376.
[28] S. Ordóñez, B.P. Vivas, F.V. Díez, Appl. Catal. B: Environ. 95 (2010) 288–296.
[29] B. Heinrichs, J.P. Schoebrechts, J.P. Pirard, J. Catal. 200 (2001) 309–320.
[30] N. Lingaiah, P.S. Sai Prasad, P.K. Rao, L.E. Smart, F.J. Berry, Appl. Catal. A: Gen. 213 (2001) 189–196.
[31] F.J. Berry, L.E. Smart, P.S. Sai Prasad, N. Lingaiah, P. Kanta Rao, Appl. Catal. A: Gen. 204 (2000) 191–201.
[32] Y. Gao, F. Wang, S. Liao, D. Yu, N. Sun, React. Funct. Polym. 44 (2000) 65–69.
[33] L. Guczi, I. Kiricsi, Appl. Catal. A: Gen. 186 (1999) 375–394.
[34] P. Bodnariuk, B. Coq, G. Ferrat, F. Fuueras, J. Catal. 116 (1989) 459–466.
[35] V. Simagina, V. Likholobov, G. Bergeret, M.T. Gimenez, A. Renouprez, Appl. Catal. B: Environ. 40 (2003) 293–304.
[36] Z. Wu, M. Zhang, Z. Zhao, W. Li, K. Tao, J. Catal. 256 (2008) 323–330.
[37] A. Yu Stakheev, L.M. Kustov, Appl. Catal. A: Gen. 188 (1999) 3–35.
[38] Rajesh Gopinath, N. Lingaiah, B. Sreedhar, I. Suryanarayana, P.S. Sai Prasad, Akira Obuchi, Appl. Catal. B: Environ. 46 (2003) 587–594.
[39] R. Gopinath, N. Seshu Babu, J. Vinod Kumar, N. Lingaiah, P.S. Sai Prasad, Catal. Lett. 120 (2008) 312–319.
[40] N. Seshu Babu, N. Lingaiah, R. Gopinath, P.S.S. Reddy, P.S. Sai Prasad, J. Phys. Chem. C 111 (2007) 6447–6453.
[41] G. Yuan, M.A. Keane, Catal. Commun. 4 (2003) 195.
[42] S.R. Wang, Y.X. Zhu, Y.C. Xie, J.G. Chen, Chin. J. Catal. 28 (2007) 676.
[43] A. Barrera, M. Viniegra, S. Fuentes, D. Gabriela, Appl. Catal B: Environ. 56 (2005) 279–288.
[44] U. Oemar, K. Hidajat, S. Kawi, Appl. Catal. A: Gen. 402 (2011) 176–187.
[45] J.F. Faudon, F. Senocq, G. Bergeret, B. Moraweck, G. Clugnet, C. Nicot, A. Renouprez, J. Catal. 144 (1993) 460–471.
[46] H.-S. Roh, K.-W. Jun, W.-S. Dong, J.-S. Chang, S.-E. Park, Y.-I. Joe, J. Mol. Catal. A: Chem. 181 (2002) 137–142.
[47] E.J. Shin, A. Spiller, G. Tavoularis, M.A. Keane, Phys. Chem. Chem. Phys. 1 (1999) 3173–3181.
[48] J.H. Sepúlveda, N.S. Fígoli, Appl. Surf. Sci. 68 (1993) 257–264.
[49] P.A. Sermon, G.C. Bond, J. Chem. Soc. Faraday Trans. I 76 (1980) 889–900.
[50] H.-Y. Lin, Y.-W. Chen, Thermochim. Acta 419 (2004) 283–290.
[51] J.T. Miller, B.L. Meyers, F.S. Modica, G.S. Lane, M. Vaarkamp, D.C. Koningsberger, J. Catal. 143 (1993) 395–408.
[52] S.K. Singh, Y. Iizuka, Q. Xu, Int. J. Hydrogen Energy 36 (2011) 11794–11801.
[53] P.K Cheekatamarla, A.M. Lane, Int. J. Hydrogen Energy 30 (2005) 1277–1285.
[54] J.C. Bertolini, P. Miegge, P. Hermann, J.L. Rousset, B. Tardy, Surf. Sci. 331 (1995) 651–658.
[55] A. Ruban, B. Hammer, P. Soltze, H.L. Skriver, J.K. Norskov, J. Mol. Catal. A: Chem. 115 (1997) 421–429.
[56] P. Lu, T. Teranishi, K. Asakura, M. Miyake, N. Toshima, J. Phys. Chem. B 103 (1999) 9673–9682.
[57] M.A. Keane, in: M.A. Keane (Ed.), Interfacial Applications in Environmental Engineering, Marcel Dekker, New York, 2003, p. 231 (Chapter 13).
[58] Bernard Coq, Francois Figueras, Coordination Chem. Rev. 178–180 (1998) 1753–1783.
[59] C.L. Prablo Argentiere, S. Nora Figoli, Ind. Eng. Chem. Res. 36 (1997) 2543–2546.
[60] M.A. Keane, G. Tavoularis, React. Kinet. Catal. Lett. 78 (2003) 11–18.
[61] L.M. Gomez-Sainero, A. Cortes, X.L. Seoane, A. Arcoya, Ind. Eng. Chem. Res. 39 (2000) 849–854.
[62] W.C. Conner, J.L. Falconer Jr., Chem. Rev. 95 (1995) 759–788.
[63] W. Juszczyk, Z. Karpinski, I. Ratajczykowa, Z. Stanasiuk, J. Zielinski, L.L. Sheu, W.M.H. Sachtler, J. Catal. 120 (1989) 68–77.
[64] L. Prati, M. Rossi, Appl. Catal. B: Environ. 23 (1999) 135.
[65] S.B. Halligudi, B.M. Devassay, A. Ghosh, V. Ravikumar, J. Mol. Catal. A 184 (2002) 175.
[66] M.A. Aramendia, V. Borau, I.M. Garcia, C. Jimenez, F. Lafont, A. Marinas, J.M. Maranas, F.J. Urbano, J. Catal. 187 (1999) 392.
[67] N. Lingaiah, P.S. Sai Prasad, P.K. Rao, F.J. Berry, L.E. Smart, Catal. Commun. 3 (2002) 391.
[68] F.J. Berry, L.E. Smart, P.S. Sai Prasad, N. Lingaiah, P.K. Rao, Appl. Catal. A 204 (2000) 191.
[69] N. Lingaiah, P.S. Sai Prasad, P.K. Rao, L.E. Smart, F.J. Berry, Appl. Catal. A 213 (2001) 189.
[70] V.A. Yakovlev, V.V. Terskikh, V.I. Simagina, V.A. Likholobov, J. Mol. Catal. A 153 (2000) 231.
[71] F.J. Urbano, J.M. Marinas, J. Mol. Catal. A: Chem. 173 (2001) 329–345.